JVI Journals.ASM.org

Marek's Disease Viral Interleukin-8 Promotes Lymphoma Formation through Targeted Recruitment of B Cells and CD4$^+$ CD25$^+$ T Cells

Annemarie T. Engel,[a] Ramesh K. Selvaraj,[b] Jeremy P. Kamil,[c] Nikolaus Osterrieder,[a] and Benedikt B. Kaufer[a]

Institut für Virologie, Freie Universität Berlin, Berlin, Germany[a]; Department of Animal Sciences, The Ohio State University, Wooster, Ohio, USA[b]; and Department of Microbiology and Immunology, Louisiana State University Health Sciences Center, Shreveport, Louisiana, USA[c]

Marek's disease virus (MDV) is a cell-associated and highly oncogenic alphaherpesvirus that infects chickens. During lytic and latent MDV infection, a CXC chemokine termed viral interleukin-8 (vIL-8) is expressed. Deletion of the entire vIL-8 open reading frame (ORF) was shown to severely impair disease progression and tumor development; however, it was unclear whether this phenotype was due to loss of secreted vIL-8 or of splice variants that fuse exons II and III of vIL-8 to certain upstream open reading frames, including the viral oncoprotein Meq. To specifically examine the role of secreted vIL-8 in MDV pathogenesis, we constructed a recombinant virus, vΔMetvIL-8, in which we deleted the native start codon from the signal peptide encoding exon I. This mutant lacked secreted vIL-8 but did not affect Meq–vIL-8 splice variants. Loss of secreted vIL-8 resulted in highly reduced disease and tumor incidence in animals infected with vΔMetvIL-8 by the intra-abdominal route. Although vΔMetvIL-8 was still able to spread to naïve animals by the natural route, infection and lymphomagenesis in contact animals were severely impaired. *In vitro* assays showed that purified recombinant vIL-8 efficiently binds to and induces chemotaxis of B cells, which are the main target for lytic MDV replication, and also interacts with CD4$^+$ CD25$^+$ T cells, known targets of MDV transformation. Our data provide evidence that vIL-8 attracts B and CD4$^+$ CD25$^+$ T cells to recruit targets for both lytic and latent infection.

Marek's disease virus (MDV) is an alphaherpesvirus that causes Marek's disease (MD), a syndrome characterized by paralysis, immunosuppression, and visceral T-cell lymphomas in chickens (10). Severity of disease is dependent on the virulence of the MDV strain and the genotype of the infected chicken (42). Infection of susceptible animals with virulent MDV strains usually results in a mortality of 70 to 100% (29). Over the years, a number of vaccines that not only prevent disease but also were the first to provide protection against a virus-induced cancer were developed (4). Since the introduction of MDV vaccination, more virulent strains that are able to overcome the vaccine hurdle have evolved, requiring the development of new vaccines to protect chickens from the disease (20).

MDV infection is initiated by inhalation of infectious dust from a contaminated environment. In the respiratory tract, virus is likely taken up by macrophages and/or dendritic cells that transport the virus to the primary lymphoid organs; however, infected B cells can be detected in the lung as early as 2 days postinfection (3). Upon transport to the primary lymphoid organs, MDV efficiently replicates in B cells and subsequently infects activated CD4$^+$ T cells that carry the virus to the feather follicle epithelium, where infectious virus is produced and shed into the environment.

MDV primarily establishes latent infection in CD4$^+$ T cells, which can become transformed, leading to lymphomagenesis (20). MDV-transformed cells have a regulatory T-cell (T_{reg}) phenotype based on their cytokine and cell surface marker profiles, which include major histocompatibility complex class II, CD30, and CD25 (7, 8, 36). However, it remains unknown whether T_{reg}s are directly infected or if infected cells instead acquire the T_{reg} phenotype during MDV-induced transformation. Several factors that contribute to MDV-induced lymphomagenesis have been identified. The major MDV oncogene is *meq*, which encodes a basic leucine zipper (bZIP) transcription factor that alters expression of cellular and viral genes. The Meq protein interacts with a number of cellular genes, including the transactivators c-Jun and c-Myc, the transcriptional corepressor C-terminal binding protein-1 (CtBP), as well as the tumor suppressor proteins p53 and RB. Interactions of Meq with its cellular targets have been shown to contribute to transformation using various analytical tools, mostly, however, the generation and testing of mutant viruses (5, 6, 20, 24–26, 31, 32). Another factor involved in lymphomagenesis is a CXC chemokine, which was originally named viral interleukin-8 (vIL-8). Previous studies have demonstrated that deletion of the entire *vIL-8* open reading frame (ORF) severely affects MDV pathogenesis and significantly reduces tumor incidence by about 90% in infected chickens (12, 30). Following these initial reports, a number of splice variants that contain vIL-8 exons II and III fused to the major oncogene Meq and to other upstream genes, including *RLORF4* and *RLORF5a*, were identified (Fig. 1A). These splice products, which lack the vIL-8 signal peptide, are expressed within infected cells *in vitro* and *in vivo* (19), demonstrating the complexity of the transcription in this genomic region. It has remained unknown, however, to what degree the secreted form of the viral chemokine vIL-8, which contains all three vIL-8 exons, and the various splice variants containing only vIL-8 exons II and III contribute to MDV pathogenesis and, especially, lymphomagenesis.

Chemokines such as vIL-8 are small, secreted proteins of 8 to 14 kDa in size which orchestrate inflammation and homeostasis by recruiting immune cells to sites of action (21, 22, 38). Initially, vIL-8 was thought to be a homologue of 9E3/CEC4 and CAF,

Received 2 March 2012 Accepted 22 May 2012
Published ahead of print 30 May 2012
Address correspondence to Nikolaus Osterrieder, no.34@fu-berlin.de, or Benedikt B. Kaufer, b.kaufer@fu-berlin.de.

doi:10.1128/JVI.00556-12

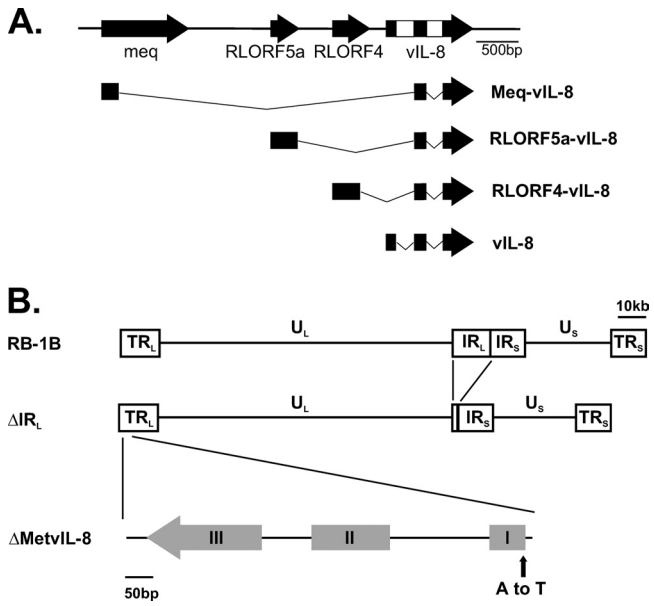

FIG 1 Overview of MDV genome and vIL-8 splice variants. (A) Schematic representation of the long repeat (R_L) region segment containing *meq*, *RLORF4*, *RLORF5a*, and *vIL-8*. Selection of splice variants of indicated genes with vIL-8 exons II and III are shown as described *in vitro* and/or *in vivo* by Jarosinski et al. (19). (B) Overview of the MDV pRB-1B genome consisting of two unique regions, long (U_L) and short (U_S), flanked by long terminal and internal repeats (TR_L and IR_L) and short terminal and internal repeats (TR_S and IR_S), respectively. Recombinant pRB-1B with a deletion of most of the IR_L ($p\Delta IR_L$) and a vIL-8 start codon mutation ($p\Delta$MetvIL-8) in the TR_L are shown.

which are members of the IL-8 family in chickens. Since the completion of the chicken genome project, several other chemokines with a higher amino acid sequence homology to vIL-8 have been identified, including members of the CXCL13 family (21, 38). Despite sequence homology, functional data will be needed to identify the bona fide cellular orthologue of vIL-8 in chickens (21, 22, 38). vIL-8 has previously been shown to attract peripheral blood mononuclear cells (PBMCs) in chemotaxis assays; however, the specific cell type(s) recruited and, hence, the function of vIL-8 in MD pathogenesis remained unknown (30).

In this study, we investigated if and how the secreted chemokine vIL-8 contributes to MDV pathogenesis. Here we show that vIL-8 is involved in lymphomagenesis and establishment of infection upon spread from infected to uninfected animals by the natural route. Furthermore, we demonstrate that vIL-8 binds to and attracts B cells, the main substrate of lytic MDV replication (11). In addition, we provide first evidence that vIL-8 interacts with and likely recruits $CD4^+$ $CD25^+$ T cells, potential targets for MDV infection and transformation.

MATERIALS AND METHODS

Cells and viruses. Chicken embryo cells (CECs) were prepared from specific-pathogen-free embryos and maintained as described previously (28). For reconstitution of recombinant viruses, CECs were transfected with purified bacterial artificial chromosome (BAC) DNA by $CaPO_4$, as described previously (17, 28, 34). Mini-F vector sequences, which are flanked by *loxP* sites in the recombinant virus genomes, were removed by cotransfection with pCAGGS-NLS/Cre, a plasmid encoding Cre recombinase (13). Virus was propagated on CECs for 2 to 4 passages, and infected cells were stored in liquid nitrogen. Virus stocks were titrated on fresh CECs. Removal of mini-F sequences in reconstituted viruses was confirmed by PCR, as described previously (17).

Generation of vIL-8 mutant viruses. vIL-8 mutant viruses were generated from pRB-1B, an infectious BAC clone of the highly oncogenic RB-1B MDV strain, using two-step Red-mediated mutagenesis, as described previously (40). Initially, approximately 10 kbp of the long internal repeat (IR_L) of pRB-1B was deleted, leaving 0.5 kbp at the left end and 1.5 kbp at the right end of the IR_L intact to allow restoration of the sequence via homologous recombination during MDV replication in this virus ($p\Delta IR_L$) (Fig. 1). In $p\Delta IR_L$, the vIL-8 start codon ATG was mutated to TTG ($p\Delta$MetvIL-8); a revertant ($p\Delta$MetvIL-8rev) was also generated. For generation of $p\Delta IR_L$, $p\Delta$MetvIL-8, and $p\Delta$MetvIL-8rev, the *aphAI*–I-SceI cassette was amplified from pEPkanS1 using primers (Table 1) containing the desired mutation and homologous sequences for both recombination events. The purified PCR product was introduced into GS1783 bacteria harboring pRB-1B or its derivatives. Positive clones were selected and screened by restriction fragment length polymorphism (RFLP) analyses with several restriction enzymes. Upon removal of the positive-selection marker, all clones were confirmed by PCR, DNA sequencing of the

TABLE 1 Primers used for construction of virus mutants

Construct	Sequence (5′–3′)[a]	Direction
ΔR_L	GTATGTGTGGGAGAAAGTATGTCGATTTTAAATGTAGTTGGTCCTGTATCTACCTATAGGTA GGGATAACAGGGTAATCGATTT	Forward
ΔR_L	CCAATAACTCGAACGCTCTTCCTATAGGTAGATACAGGACCAACTACATTTAAAATCGACGC CAGTGTTACAACCAATTAACC	Reverse
IR_L deletion	CGAACGGAATGTACAACAGCTTGC	Forward sequencing
IR_L deletion	GATAAGACACTTTCCCACTCATAC	Reverse sequencing
ΔMetvIL-8	GCAGGGGGTGTGGGTTTGATGAGCAGTTGGGGCGGCAAAA**T**TGCAGGCGTTGTTGCTAGTAT TGGTAGGGATAACAGGGTAATCGATTT	Forward
ΔMetvIL-8	CAAATAGATCTGTACTATGAATAGAACCAATACTAGCAACAACGCCTGCA**A**TTTTGCCGCCCC AACTGCTCATCGCCAGTGTTACAACCAATTAACC	Reverse
ΔMetvIL-8rev	TGTACTATGAATAGAACCAATACTAGCAACAACGCCTGCA**T**TTTTGCCGCCCCAACTGCTAGT GTTACAACCAATTAACC	Forward
ΔMetvIL-8rev	GCAGGGGGTGTGGGTTTGATGAGCAGTTGGGGCGGCAAAA**A**TGCAGGCGTTGTTGCTAGTG ATAACAGGGTAATCGATTT	Reverse
vIL-8 seq	CTGCTATGCAGGGGTCGTGGGAA	Forward sequencing
vIL-8 seq	GCACCTCTTGTCGACAGCGAGAC	Reverse sequencing

[a] Mutated sequences are shown in bold letters.

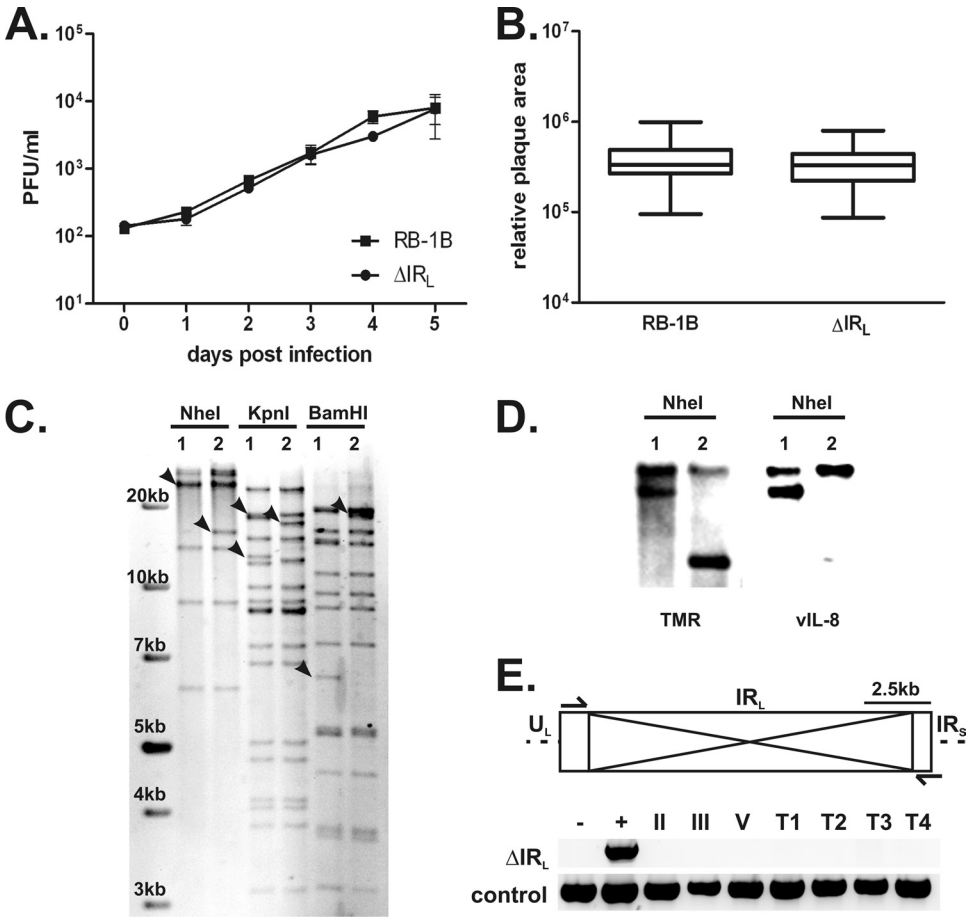

FIG 2 Characterization of vΔIR_L. (A) Multistep growth kinetics of recombinant viruses vRB-1B and vΔIR_L are shown with the SEM for one experiment with triplicates. (B) Plaque area analysis of vRB-1B and vΔIR_L ($n = 150$; Mann-Whitney U test, $P > 0.05$) Plaque sizes are shown as means with 95% confidence intervals and SDs. (C) RFLP analysis of pRB-1B (lanes 1) and pΔIR_L (lanes 2) with the indicated restriction enzymes. Expected changes are indicated by arrowheads. (D) Southern blot of an NheI digest of pRB-1B (lanes 1) and pΔIR_L (lanes 2). Fragments containing the R_L were detected with digoxigenin-labeled probe specific for vIL-8 or viral TMRs present in the R_L adjacent to the deletion. (E) Restoration of the IR_L in vΔIR_L-infected cells *in vitro* and *in vivo*. Schematic representation of the IR_L in the MDV genome. Deleted sequences and primers used for the PCR analyses are indicated. (Top) The deletion site was amplified from DNA extracted from infected CECs at 2 (II), 3 (III), or 5 (V) passages after virus reconstitution, as well as from 4 different tumor tissues (T1 to T4). pRB-1B served as a a negative control (lane −), and pΔIR_L served as a positive control (lane +). (Bottom) The quality of all DNA samples was tested by a control PCR using the vIL-8 sequencing primer.

targeted region (Fig. 1B), as well as multiple RFLP analyses to ensure the integrity of the genome.

Southern blotting. To visualize deletion of IR_L, pRB-1B and pΔIR_L DNA was digested with NheI, separated by agarose gel electrophoresis, and transferred onto a Nytran SuPerCharge (SPC) membrane (Whatman). Bands containing the IR_L were detected using digoxigenin-labeled probes specific for the *vIL-8* gene or viral telomeric repeats (TMRs) (23). Probes were visualized using alkaline phosphatase-conjugated antidigoxigenin antibodies and the CDP Star system (Roche Applied Science). Images were recorded with a Chemi-Smart 5100 detection system (PeqLab).

Growth kinetics and plaque size assays. Replication properties of recombinant viruses were determined by multistep growth kinetics as described previously (35). Briefly, 1×10^6 CECs were infected with 100 PFU of each recombinant virus. At days 1, 2, 3, 4, 5, and 6 postinfection (p.i.), cells were harvested, titrated on fresh CECs, and fixed at 6 days p.i. with 90% ice-cold acetone. For plaque size assays, 1×10^6 CECs were infected with 100 PFU and fixed at 6 days p.i. Fixed cells were stained with anti-MDV chicken serum, and plaques were visualized using an anti-chicken Alexa Fluor 488 secondary antibody. Images of at least 45 randomly selected plaques were taken, and plaque areas were determined using Image J software (NIH).

Analysis of ΔIR_L restoration. DNA was isolated from CECs infected with vΔIR_L at passages 2, 3, and 5 after virus reconstitution as well as tumor cells derived from animals that had been infected with vΔIR_L. PCR was performed using primers specific for the IR_L deletion site (Fig. 2D) or for vIL-8, which was included as a control (Table 1).

Western blot analysis of vIL-8 expression. CECs (1×10^6) were infected with 500 PFU of parental virus with the IR_L deletion (vΔIR_L), vΔMetvIL-8, or vΔMetvIL-8rev. Supernatants from infected cells were harvested at 6 days p.i. and resolved on sodium dodecyl sulfate (SDS)-gradient polyacrylamide gel electrophoresis (PAGE) gels, and proteins were transferred to a polyvinylidene difluoride membrane in a semidry blot system at 1.2 mA/cm^2 for 40 min. Membranes were then probed using a polyclonal rabbit anti-vIL-8 antibody or mouse monoclonal anti-glycoprotein C (anti-gC) antibody (clone 1A6) kindly provided by Jean-Francois Vautherot (INRA, Nouzilly, France) at 1:5,000 and 1:100 dilutions, respectively (12, 39). Target proteins were visualized using a horseradish peroxidase-conjugated goat antirabbit antibody and goat anti-mouse IgM (Southern Biotech), each at a 1:10,000 dilution, using enhanced chemiluminescence (ECL) Plus Western blot detection reagents (Amersham GE Healthcare), and the signal was recorded using a Chemi-Smart 5100 detection system (PeqLab).

Detection of Meq–vIL-8 splice variants. CECs were infected with vΔIR$_L$, vΔMetvIL-8, or vΔMetvIL-8rev, RNA was isolated using an RNeasy kit (Qiagen), and DNA was removed using genomic DNA eliminator columns provided by the manufacturer. RNA was transcribed into cDNA using an enhanced avian HS reverse transcription kit (Sigma). Splice products were amplified by PCR using primers as previously described (19) (Table 1). Meq–vIL-8 and vIL-8 splice products were separated by agarose gel electrophoresis and detected using a Bio-Vision detection system (PeqLab).

***In vivo* experiments.** One-day-old (experiment 1 [Exp 1]) or 2-day-old (experiment 2 [Exp 2]) specific-pathogen-free Valo chickens (Lohmann Tierzucht, Germany) were infected intra-abdominally with 1,000 PFU of either vΔIR$_L$, vΔMetvIL-8, or vΔMetvIL-8rev. Naïve chickens were housed with infected animals to investigate transmission of the virus via the natural route of infection. Chickens were monitored for clinical symptoms of MD on a daily basis. Animals were examined for tumorous lesions postmortem, once clinical symptoms were evident or after termination of the experiments. Exp 1 was terminated at 63 days p.i., and Exp 2 was terminated at 91 days p.i. Stability of the vIL-8 start codon mutation was confirmed by DNA sequencing of the vIL-8 locus derived from vΔMetvIL-8-induced tumors.

Quantification of MDV genome copies in chicken whole blood. Blood samples were taken from infected animals at 4, 7 10, 14, 21, and 28 days p.i. and from contact animals at 35 and 40 days p.i. to determine the number of MDV genome copies in the blood. DNA was isolated using an E-Z96 96-well blood DNA isolation kit (Omega Biotek) according to the manufacturer's instructions. The number of MDV genome copies was determined by quantitative PCR (qPCR) using specific primers and a probe for the gene encoding MDV ICP4. ICP4 copy numbers were normalized against the numbers of cellular genome copies of the inducible nitric oxide synthase (iNOS) gene as described previously (16–18).

Expression of recombinant vIL-8. Recombinant vIL-8 protein was generated using a Bac-to-Bac baculovirus expression system (Invitrogen). Briefly, the vIL-8 gene was expressed as a secreted protein, vIL-8–Fc–His, bearing a C-terminal tag comprised of the Fc region of human immunoglobulin G (IgG), followed by a polyhistidine motif (6×His). To generate recombinant baculovirus expressing vIL-8–Fc, the vIL-8 cDNA was first PCR adapted and cloned into the CpoI site of pFastBac11-Cpo-Fc-His, a derivative of pFastBac11-Cpo-His (41), which incorporates an IgG Fc cDNA from pcDNA-IgG Fc (a generous gift of O. Negrete and B. Lee, University of California, Los Angeles, Los Angeles, CA) (27, 41). The vIL-8–Fc–His vector enabled construction of baculovirus expressing vIL-8 with an Fc-His tag, while the empty vector allowed construction of baculovirus expressing the Fc-His-only control protein. Recombinant bacmid DNA was generated from pFastBac constructs using the Bac-to-Bac system, as per the manufacturer's instructions, and transfected into Sf9 insect cells. Baculoviruses were propagated and titrated on Sf9 cells, and expression of the recombinant vIL-8–Fc–His and Fc-His protein from the recombinant baculoviruses was confirmed by Western blotting. Recombinant vIL-8–Fc–His and Fc-His were purified by protein G affinity chromatography. Supernatant from infected Sf9 cells was harvested at 72 to 96 h postinfection, diluted 1:2 with binding buffer (20 mM NaH_2PO_4, pH 7.0), and applied to a protein G column (Pierce). The column was washed with binding buffer, and target proteins were eluted with elution buffer (0.1 M glycine, pH 3) and neutralized with 1 M Tris, pH 9 (2). Recombinant protein was analyzed by Western blotting as described above, and purity was determined by Coomassie brilliant blue staining. Fractions containing pure vIL-8–Fc–His or Fc-His were collected, protein concentrations were determined using the Bradford assay (Pierce), and aliquots were stored at −80°C.

Isolation of chicken PBMCs. Chicken PBMCs were prepared from fresh chicken blood, kindly provided by the Institut für Geflügelkrankheiten of the Freie Universität Berlin, and stored until processing in sodium citrate buffer. PBMCs were isolated from the blood using a Bicoll 1.077-g/ml gradient (Biochrom) according to the manufacturer's instructions.

Binding assay and flow cytometry. One million cells were incubated with vIL-8–Fc–His or Fc-His (250 nM) and stained with mouse anti-Bu1, mouse anti-chicken CD4, or anti-chicken CD8 antibodies (Southern Biotech), each at a 1:500 dilution. Secondary anti-human Fc (huFc)-Cy5, anti-mouse IgG Alexa Fluor 488 (Fab fragment), and anti-mouse IgM-fluorescein isothiocyanate antibodies were used at dilutions of 1:1,000. CD25 staining was performed as the last step of the staining procedure using a phycoerythrin-labeled mouse anti-CD25 antibody at a 1:100 dilution (37). Stained cells were fixed with 0.5% paraformaldehyde (PFA) and analyzed using a FACScalibur flow cytometer (BD Bioscience), and data were evaluated using FlowJo software (Tree Star Inc.).

Chemotaxis assay. Freshly isolated PBMCs were resuspended in chemotaxis medium (RPMI 1640, 0.25% bovine serum albumin) at a concentration of 1×10^6 cells/ml. Chemotaxis assays were performed as described previously (13) using transwell plates with 5-μm-pore-size polycarbonate membranes (Corning Costar) according to the manufacturer's instructions. Briefly, vIL-8–huFc–His, huFc-His, or 9E3/CEF4 was diluted to 50 nM in chemotaxis medium, and 600 μl was added to the lower chamber. Fibronectin (5 μg/ml) served as a positive control. PBMCs (1×10^5) were added to the upper chamber, and the plates were incubated for 40 min at 42°C. Migrated cells and input cells were measured for 30 s or 120 s at a constant flow rate by flow cytometry as described previously (8).

Characterization of migrated cells. To determine the cell populations that migrate in chemotaxis assays, 100 μl of the cells in the lower chamber was settled on polylysine slides for 3 h, washed with phosphate-buffered saline containing 1% fetal calf serum, and fixed with 0.5% PFA at 4°C. Slides were stained with mouse anti-Bu1, -CD4, -CD8, or -CD25 antibodies at 1:500 dilutions and visualized using Alexa Fluor 488 anti-mouse IgG antibodies (Invitrogen) at 1:1,000 dilutions. Slides were mounted with DAPI (4′,6-diamidino-2-phenylindole; VectaShield; Vector Laboratories Inc.), images were taken with an Axiovert M1 microscope system (Zeiss), and the number of B, $CD4^+$, or $CD8^+$ T cells was determined for each sample using AxioVision software (Zeiss).

Statistical analysis. Statistical analysis was performed using SPSS software (IBM). Plaque size data for recombinant MDV were analyzed using the Mann-Whitney U test and one-way analysis of variance (ANOVA). Data on the number of MDV genome copies in whole-blood samples were analyzed using Kruskal-Wallis and Mann-Whitney U tests. Tumor incidence was analyzed using Fisher's exact and Fisher-Freeman-Hamilton tests (StatXact software). Results from chemotaxis and migration assays were analyzed by one-way ANOVA.

RESULTS

Generation and characterization of a vIL-8 start codon mutant. Previously, a recombinant MDV lacking the entire vIL-8 ORF was shown to be unable to efficiently produce lymphomas in inoculated chickens. However, it remained unclear whether this defect was caused by the absence of the vIL-8 chemokine or of one or more of the splice variants that vIL-8 exons II and III form with Meq, *RLORF4*, and *RLORF5a* (Fig. 1A) (19). To determine to what extent the secreted vIL-8 contributes to MDV pathogenesis, we introduced a point mutation in the vIL-8 start codon to abrogate its expression without affecting splicing with other genes. In the MDV genome, two copies of the *vIL-8* gene are present, one in each of the long repeat sequences (R_L), both of which have to be mutated to abrogate its expression. However, targeting a locus in the R_L often poses a technical challenge and requires massive screening of numerous clones. To facilitate mutagenesis of *vIL-8*, we deleted most of the long internal repeat region (ΔIR_L) containing vIL-8 in pRB-1B (pΔIR$_L$; Fig. 1B) (40). RFLP analyses of pRB-1B and pΔIR$_L$ with various restriction enzymes and Southern blotting using probes specific for vIL-8 or the viral TMRs (Fig.

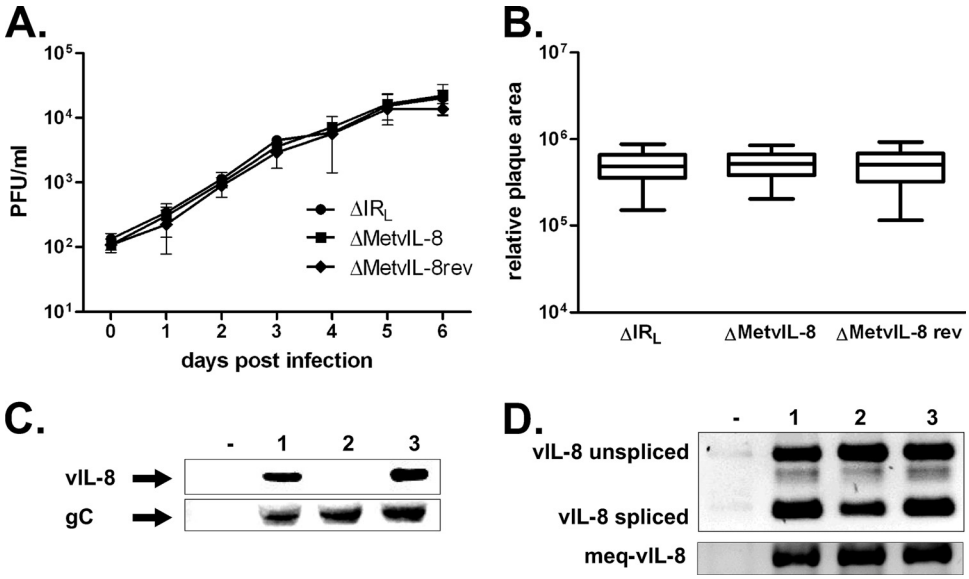

FIG 3 Mutation of the vIL-8 start codon abrogates vIL-8 expression but does not affect MDV replication or splicing in the region. (A) Multistep growth kinetics of vΔIR$_L$, vΔMetvIL-8, and vΔMetvIL-8rev shown as geometric means with SEMs for one experiment with triplicates. (B) Plaque size assay of vΔIR$_L$, vΔMetvIL-8, and vΔMetvIL-8rev ($n = 135$; one-way ANOVA, $P > 0.05$). Plaque sizes are shown as means with 95% confidence intervals and SDs. (C) Western blot analysis detecting vIL-8 (top) or gC (bottom) in the supernatant of CECs infected with the indicated viruses. (D) Analysis of vIL-8 (top) and Meq–vIL-8 (bottom) splicing by PCR in CECs infected vΔIR$_L$ (lane 1), vΔMetvIL-8 (lane 2), or vΔMetvIL-8rev (lane 3). Splice products described previously by Jarosinski et al. (19) are indicated.

2C and D) confirmed the expected changes in the respective recombinants. To determine if the deletion of the IR$_L$ had an effect on MDV replication and pathogenesis, we tested the mutant *in vitro* and *in vivo*. Multicycle growth kinetics and plaque size assays showed that vΔIR$_L$ replicates comparably to parental vRB-1B (Fig. 2A and B). Furthermore, vΔIR$_L$ induced disease and lymphomas *in vivo* at rates comparable to those for the parental vRB-1B (data not shown). To determine if IR$_L$ was restored during vΔIR$_L$ replication in cultured cells, we isolated DNA from various passages after virus reconstitution and growth in CECs and from tumor tissues and PCR amplified a sequence specific for the ΔIR$_L$ region as well as vIL-8, which is also present in the left terminal repeat (TR$_L$) as a control (Fig. 2D). While the deletion was clearly present in the ΔIR$_L$ bacmid, the repeat region was rapidly repaired during virus replication as early as 2 passages after reconstitution and was also restored in tumor cells derived from chickens infected with the ΔIR$_L$ virus.

Next, we mutated the vIL-8 start codon (pΔMetvIL-8) in the remaining R$_L$ copy of pΔIR$_L$, to determine the role of the secreted chemokine. Reconstitution of pΔMetvIL-8 resulted in viable virus (vΔMetvIL-8) that replicated in a fashion that was comparable to that of parental and revertant viruses (vΔMetvIL-8rev), as evidenced in multicycle growth kinetics and plaque size assays *in vitro* (Fig. 3A and B). To confirm that splicing is not affected by mutation of the vIL-8 start codon, we analyzed vIL-8 and Meq–vIL-8 splice variants in vΔMetvIL-8-infected CECs. Both vIL-8 and Meq–vIL-8 were efficiently spliced in vΔMetvIL-8-infected cells, and levels were comparable to those of parental and revertant viruses (Fig. 3D). We concluded from the experiments that mutating the vIL-8 start codon did not affect splicing in this region.

To confirm that the vIL-8 start codon mutation indeed resulted in loss of vIL-8 expression and secretion, we performed Western blot analysis to detect the vIL-8 protein in cell culture supernatants of infected CECs (Fig. 3C). Supernatants from vΔMetvIL-8-infected cells did not contain vIL-8, while the chemokine was readily detectable in cells infected with parental or revertant virus. The secreted MDV gC used as a control for a secreted MDV gene product was detectable in all infected cells, which confirmed that the mutation affected only the targeted gene.

The secreted chemokine vIL-8 plays a role in MDV pathogenesis. To elucidate if secreted vIL-8 is involved in MDV pathogenesis and lymphomagenesis, we infected 1- or 2-day-old Valo chickens with vΔIR$_L$, vΔMetvIL-8, or vΔMetvIL-8rev and monitored them for 63 days or 91 days in two independent experiments. To analyze MDV lytic replication, we performed qPCR analysis on DNA from whole blood of infected chickens. The numbers of MDV genome copies of vΔMetvIL-8 were reduced in one experiment compared to those observed after infection with parental and revertant viruses (Fig. 4A and B). Furthermore, we monitored disease development over the course of the experiments. Only 46% (Exp 1) and 42% (Exp 2) of the chickens infected with vΔMetvIL-8 developed MD, while 92% (ΔIRL) and 100% (ΔMetvIL-8rev) succumbed to disease at the termination of the experiments, indicating that secreted vIL-8 contributes to MDV pathogenesis (Fig. 4C and D). Total tumor incidence after final necropsies was also reduced to 70% and 42% in Exp 1 and Exp 2, respectively (Fig. 4E and F). To determine if a reversion of the start codon mutation in vΔMetvIL-8 was responsible for the residual lymphomagenesis in infected animals, we isolated DNA from tumor cells and sequenced the vIL-8 region. Sequence analysis confirmed that the start codon mutation was present in all vΔMetvIL-8-induced tumors (data not shown), indicating that the mutation was stable *in vivo*. Taken together, our data demonstrated that abrogation of vIL-8 expression severely attenuates viral pathogenesis and lymphomagenesis in MDV.

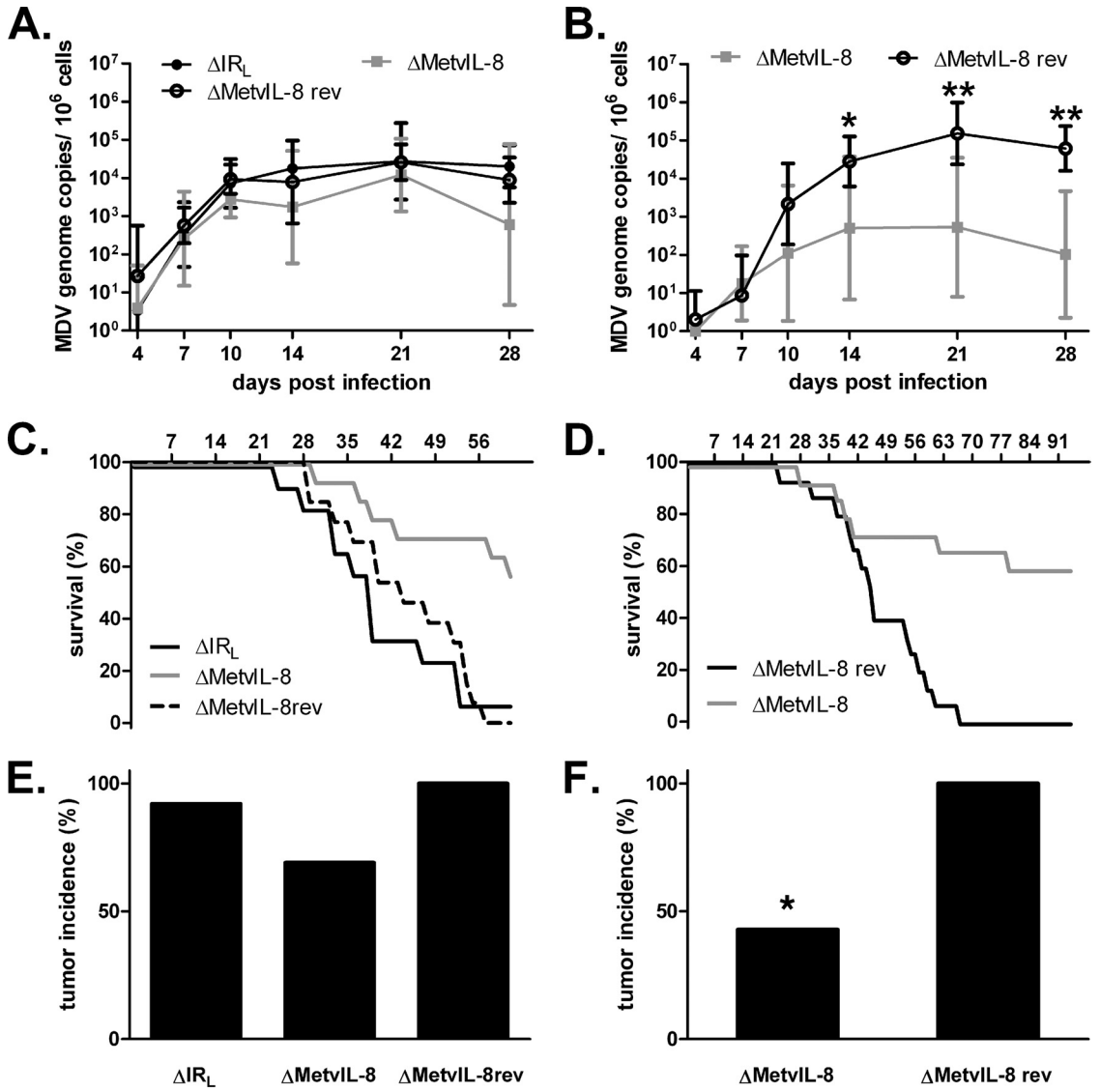

FIG 4 vIL-8 expression is dispensable for lytic replication but impairs disease development and tumor formation *in vivo*. (A and B) qPCR analysis of the viral ICP4 gene and host iNOS gene. Blood samples of animals infected with ΔIR_L, vΔMetvIL-8, or vΔMetvIL-8rev were taken at 4, 7, 10, 14, 21, and 28 days p.i. Mean MDV genome copy numbers per 1×10^6 cells of eight infected chickens per group are shown. Viral titers in the blood in Exp 1 (A) (Kruskal-Wallis test, $P > 0.05$; $n = 24$ for all time points) and Exp 2 (B) (Mann-Whitney U test, $P = 0.01$ for 14 days p.i. and $P = 0.002$ for 21 and 28 days p.i.; $n = 24$ for all time points) decreased in vΔMetvIL-8-infected animals compared to vΔMetvIL-8rev-infected animals. (C and D) Survival analysis of chickens infected with indicated viruses during Exp 1 (C) and Exp 2 (D). (E and F) Tumor incidence in chickens infected with the indicated viruses. Necropsies were performed on chickens upon onset of clinical symptoms or after termination of the experiment. Tumor incidence is shown as a percentage of animals per group. (E) Exp 1 (Fisher-Freeman-Hamilton test, $P = 0.32$); (F) Exp 2 (*, Fisher's exact test, $P = 0.001$).

vΔMetvIL-8 is severely impaired for the establishment of infection in contact chickens. To determine if vIL-8 is involved in the establishment of MDV infection via the natural route of infection, we housed naïve chickens with vΔMetvIL-8- or vΔMetvIL-8rev-infected animals in the second experiment. Even though vΔMetvIL-8 was able to spread to naïve chickens, MDV genome copies were detectable only at low levels in the blood of only a few vΔMetvIL-8-contact animals. In virus-positive chickens, MDV loads in the blood were decreased by more than 1,000-fold in vΔMetvIL-8-contact chickens compared to those in animals infected with revertant virus (Fig. 5A). Furthermore, viral loads in the blood of vΔMetvIL-8-contact chickens increased only slightly over time, suggesting that the establishment of MDV infection is severely impaired in the absence of the secreted vIL-8 chemokine. To confirm these findings, we monitored disease incidence over the course of the experiment. None of the ΔMetvIL-8-contact chickens developed disease over the 91 days of the experiment, while the revertant virus induced severe disease in most of the contact animals (Fig. 5B). Similarly, at the termination of the experiment, only 1 out of 10 contact chickens showed minor lesions in the testes at necropsy, while 50% of animals infected with the revertant virus had tumorous lesions in multiple organs. Taken together, our data demonstrated that the secreted chemokine is essential for the establishment of MD via the natural route.

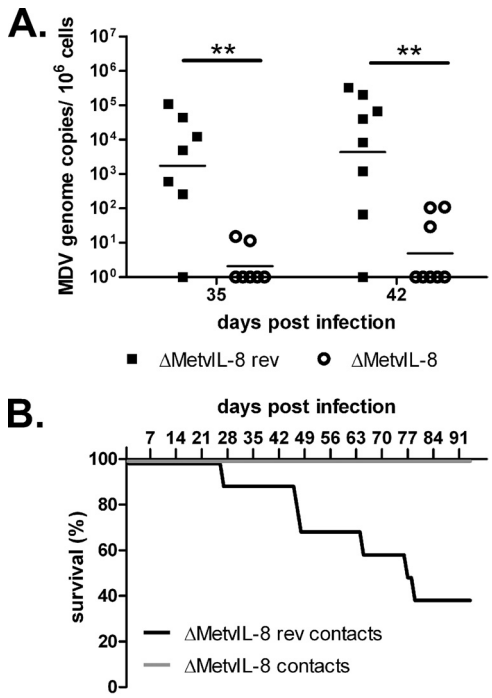

FIG 5 Disease and tumor development in animals infected via the natural route of infection. (A) qPCR of MDV genome copies in the blood of chickens infected with the indicated virus via the natural route of infection. Geometric means of MDV genome copies per 1×10^6 cells are shown for 35 and 42 dpi ($n = 24$; Mann-Whitney U test, $P = 0.007$ for 35 and 42 days p.i.). (B) Survival analysis of contact birds infected with the indicated viruses.

vIL-8 binds to and attracts B cells. Parcells and colleagues previously reported that vIL-8 attracts a fraction of chicken PBMCs but did not identify the PBMC subset (30). To elucidate precisely which cell populations are recruited by vIL-8, we expressed recombinant vIL-8–Fc–His (Fig. 6A) using a baculovirus expression system and performed *in vitro* binding and chemotaxis assays. Binding assays revealed that vIL-8–Fc–His, but not the Fc-His control protein (Fig. 6B, left), bound to B cells, which represent the main target of MDV lytic replication (10). Besides B cells, vIL-8–Fc–His also interacted with about 10% of $CD4^+$ T cells, but not with $CD8^+$ T cells (Fig. 6B, middle and right). To test if vIL-8 could also induce cell migration, we performed chemotaxis assays with chicken PBMCs. vIL-8–Fc–His efficiently induced chemotaxis of PBMCs, resulting, on average, in a 3- to 4-fold increase in migration compared to that for the Fc-His control protein or 9E3/CEF4, a chemokine that mainly attracts monocytes and macrophages (Fig. 6C) (9). To determine the PBMC subset that migrated in the presence of vIL-8–Fc–His, we fixed migrated cells on polylysine slides and stained for B-cell as well as $CD4^+$ and $CD8^+$ T-cell markers. The percentage of B cells was significantly increased in the presence of vIL-8, while B-cell ratios were not altered using the Fc-His control protein compared to the input control (Fig. 6D). In contrast, we did not observe a significant difference in the percentage of $CD4^+$ or $CD8^+$ T cells in the presence of vIL-8–huFc–His. Our data demonstrated that vIL-8 is able to bind to and recruit B cells, suggesting that vIL-8 expression of infected cells *in vivo* could aid the recruitment of B cells to the site of infection.

vIL-8 interacts with $CD4^+$ $CD25^+$ T cells. In our binding assays (Fig. 6B), we observed that a small subset of $CD4^+$ T cells bound to vIL-8–Fc–His. Since $CD4^+$ T cells are the target for latent MDV infection and transformation, we decided to further characterize this population. As MDV tumor cells have previously been shown to mainly consist of T cells with a regulatory phenotype (37), we determined if $CD4^+$ $CD25^+$ T cells can bind vIL-8–Fc–His. Strikingly, all $CD25^+$ cells were able to bind vIL-8–Fc–His (Fig. 7A). Furthermore, we could demonstrate that vIL-8–Fc–His strongly labeled $CD4^+$ $CD25^+$ T cells to the point that virtually all of these cells appeared to bind vIL-8–Fc–His in our assays, suggesting that these cells could be recruited to the site of infection *in vivo* by secreted vIL-8 (Fig. 7B).

DISCUSSION

In this study, we investigated the role of the secreted vIL-8 chemokine in MDV pathogenesis. Furthermore, we interrogated how this viral chemokine can modulate the immune system to aid the establishment of MDV infection and lymphomagenesis. Previously, it was reported that deletion of the entire vIL-8 ORF in the MDV genome resulted in viruses that were severely impaired with respect to lymphomagenesis and disease induction (12, 30). Moreover, a *vIL-8* deletion mutant efficiently replicated in feather follicle epithelium, spread to naïve animals, and induced high antibody titers in contact chickens (12). Intriguingly, Jarosinski and Schat discovered that vIL-8 exons II and III are not only part of the secreted chemokine but also part of a fusion protein derived from splice variants that also include the upstream genes *meq*, *RLORF4*, and/or *RLORF5a* (Fig. 1A) (19). The data raised the question about extent to which the secreted vIL-8 chemokine or the splice variants contribute to the observed phenotype of *vIL-8* deletion viruses. Anobile and colleagues reported that Meq–vIL-8 localizes to the nucleoplasm, nucleoli, and Cajal bodies (1). Moreover, Meq–vIL-8 is able to form homodimers and shows distinct mobility patterns that differ from the pattern of Meq, suggesting that the splice variants may indeed have a biological relevance (1). Furthermore, an exon I deletion mutant was previously generated to determine the role of the secreted vIL-8 chemokine by itself. This mutant virus exhibited a defect in lytic replication when chickens were infected at the age of 2 days and resulted in an MD incidence of only about 40%, suggesting that vIL-8 contributes to MDV pathogenesis, but not to such a great degree as was seen in the mutant in which the entire *vIL-8* ORF was removed (19). However, *in silico* predictions (Human Splicing Finder, version 2.4.1) (15) indicated that a branch point and three potential splice acceptor sites with high consensus values are present in exon I of vIL-8. Therefore, in this study we generated a mutant, vΔMetvIL-8, that does not interfere with splicing in the region. We observed that vΔMetvIL-8 shows a reduced potential to induce disease and lymphoma incidence compared to wild-type and revertant virus, but vΔMetvIL-8 is more pathogenic than complete *vIL-8* deletion mutants, which induce tumors in only ~10% of the chickens (30). Our results are therefore consistent with data obtained from the exon I deletion mutant that had a similar phenotype (19). Our data, taken together with those from other groups, argue that vIL-8 plays an important role in MD pathogenesis but that the previously published *vIL-8* deletion mutant likely exhibited a composite phenotype, perhaps due to effects on the transcriptional program and/or splice variants and not solely due to abrogation of vIL-8 expression. Further studies will be needed to determine if and to what extent the various vIL-8 splice variants

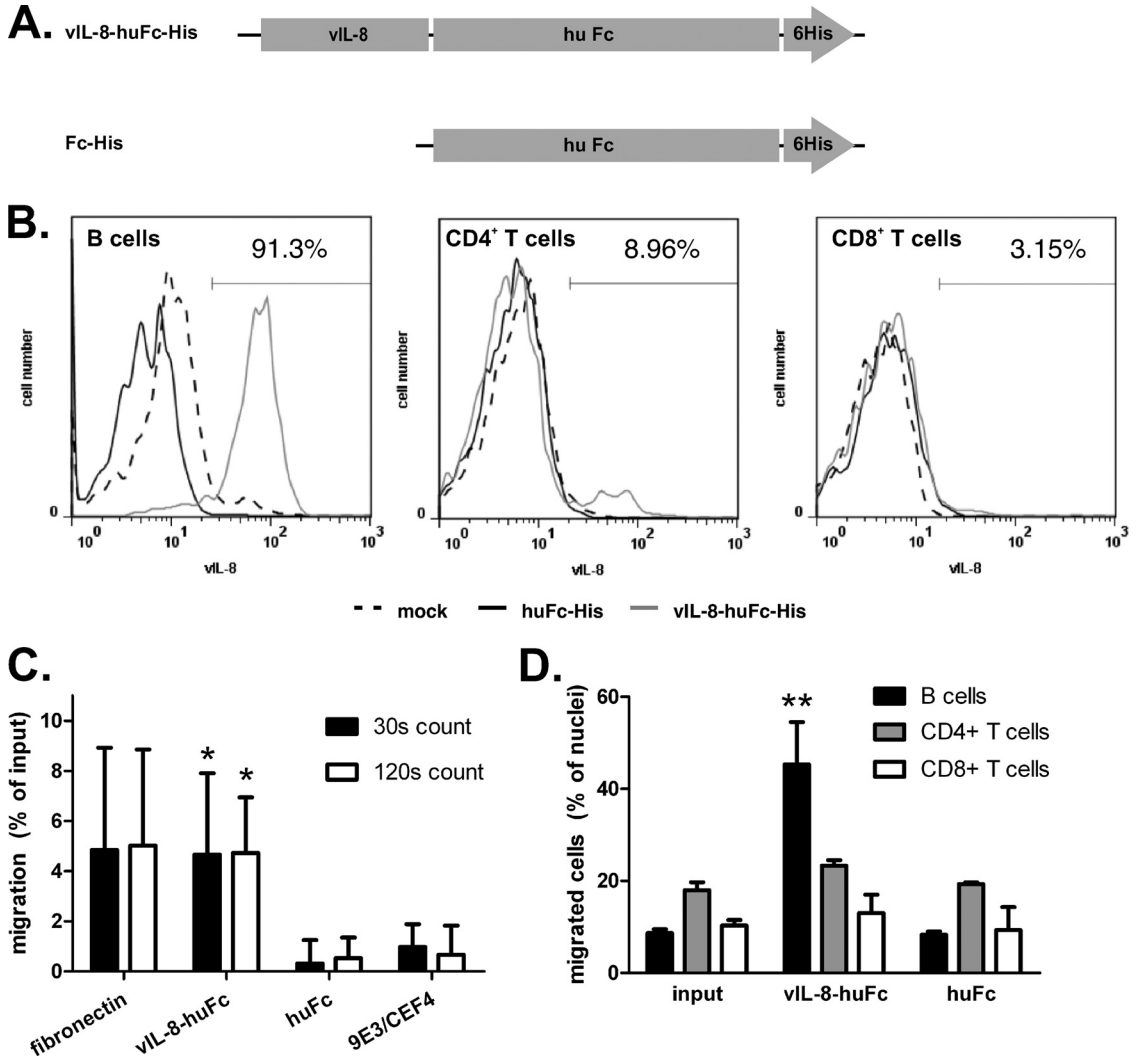

FIG 6 vIL-8 binds to and attracts B cells. (A) Recombinant proteins used for binding and chemotaxis assay produced using the baculovirus expression system. (B) Binding assay of recombinant vIL-8 to B cells (left), $CD4^+$ T cells (middle), or $CD8^+$ T cells (right). Data are shown as histograms and are representative for three independent experiments. The percentage of vIL-8-positive cells is indicated. (C) Chemotaxis assay using vIL-8 as a chemoattractant for chicken blood PBMCs. Migrated cells were counted for the indicated time intervals by flow cytometry. Data are shown as a percentage of input cells normalized against background migration. Mean of 4 independent experiments (*, for count at 30 s [$n = 12$], $P = 0.042$ [vIL-8 versus Fc] and $P = 0.089$ [vIL-8 versus 9E3/CEF4]; for count at 120 s [$n = 12$], $P = 0.011$ [vIL-8 versus Fc] and $P = 0.013$ [vIL-8 versus 9E3/CEF4] [P values by Bonferroni correction]). (D) Analysis of cells that migrated in chemotaxis assays. Data are presented as the mean percentage of B cells or $CD4^+$ or $CD8^+$ T cells for each sample from three independent experiments (**, for B cells, $P = 0.008$; for $CD4^+$ T cells, $P > 0.05$; for $CD8^+$ T cells, $P > 0.05$ [P values by Bonferroni correction for vIL-8–huFc compared to either input or huFc]).

or potential regulatory sequences contribute to the pathogenesis of MDV.

Parcells and coworkers (30) and others (12, 19) hypothesized that vIL-8 might recruit target cells to facilitate viral spread, a process that likely plays an important role during the early stages of infection. We were able to detect vΔMetvIL-8 in contact chickens, but only at very low levels. Our results therefore suggest that vIL-8 is important for the establishment of infection or for efficient spread or shedding of infectious virus.

To facilitate the generation of recombinant viruses harboring mutations in the MDV R_L region, we deleted most of IR_L in pRB-1B (pΔIR_L), leaving only the terminal sequences of ~0.5 kb and ~1.5 kb intact. vΔIR_L replicated and induced disease with an efficiency that was comparable to that of the parental virus. More importantly, the deleted IR_L sequences were completely restored after two passages in cultured cells after reconstitution, and mutations introduced into TR_L are therefore copied into the IR_L locus in the course of virus replication. Our data therefore suggest that the vΔIR_L mutant may be a versatile platform for a rapid manipulation of genes located in the R_L regions of the MDV genome.

vIL-8 had already been shown to induce chemotaxis of an unidentified subpopulation of PBMCs, suggesting that MDV might recruit specific cell types to the site of infection, which could play important roles during viral pathogenesis. Sequence alignment of vIL-8 with other chemokines revealed a homology to the B-lymphocyte chemoattractant or chicken CXCL13 family members (14, 21). Our data imply that B and $CD4^+$ $CD25^+$ T cells carry an unidentified vIL-8 receptor(s) which induces chemotaxis upon

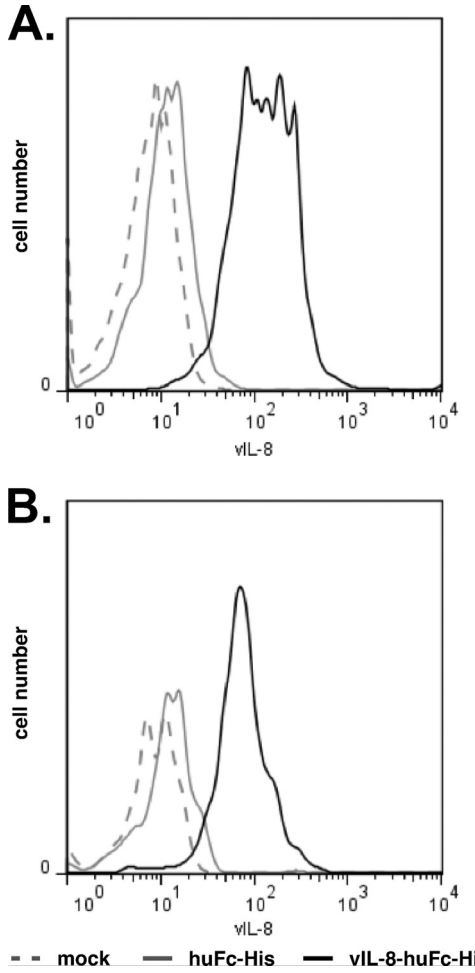

FIG 7 $CD25^+$ cells and $CD4^+$ $CD25^+$ T cells bind vIL-8. (A) Binding assay of recombinant vIL-8 to CD25-expressing cells. vIL-8 fluorescent intensity is shown for $CD25^+$ cells in the histogram. Data are representative for three independent experiments. (B) Binding assay of recombinant vIL-8 to $CD4^+$ $CD25^+$ T cells. vIL-8 fluorescent intensity is shown for $CD4^+$ $CD25^+$ T cells in the histogram. Data are representative for three independent experiments.

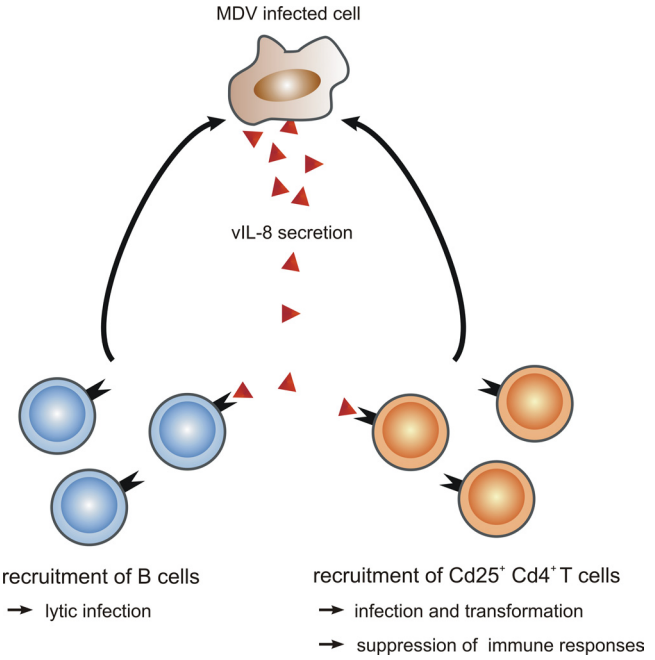

FIG 8 Model of vIL-8 functions during MD pathogenesis. vIL-8 is able to bind and recruit B cells to the site of infection, leading to the lytic infection of B cells that is necessary for efficient MDV replication in infected animals. Furthermore, vIL-8 can bind and attract $CD4^+$ $CD25^+$ T cells that could serve as a target for MDV transformation. In addition, recruitment of $CD4^+$ $CD25^+$ T cells to tumor tissue could suppress immune responses at the site of infection.

binding to vIL-8. Strikingly, vIL-8 bound and induced migration of B cells, the main target of MDV lytic replication (11). MDV-infected B cells can be detected as early as 2 days after inhalation of the virus in the lung (3). Thus, it is tempting to speculate that the vIL-8 chemokine might recruit B cells to the initial site of infection in the lung. Furthermore, the well-known delay in disease progression in the absence of B cells, e.g., upon bursectomy, underscores that B cells play a central role during early infection (3, 33). The lack of B-cell recruitment in vΔMetvIL-8-infected chickens could explain the reduced viral load in chickens infected via the natural route. Reduced levels of infected B cells in the absence of vIL-8 might, therefore, result in a less efficient infection of $CD4^+$ T cells and, as such, decrease the likelihood of T-cell transformation and lymphomagenesis.

Previous studies demonstrated that primary MDV tumor cells have a T_{reg} phenotype, as transformed cells were shown to express well-established markers of regulatory T cells such as CD4 and CD25 (7, 36). In this study, we were able to demonstrate that vIL-8 specifically binds to $CD4^+$ $CD25^+$ T cells, which suggests that vIL-8 might recruit these cells as a target for infection and transformation. As CD25 is a component of the IL-2 receptor (IL-2R), which promotes cell proliferation and increased viability of naïve T cells, it is possible that IL-2R signaling is subverted in the initial stages of transformation and immortalization, resulting in lymphomagenesis (7). Alternatively, it is tempting to speculate that the recruited $CD4^+$ $CD25^+$ T cells have a regulatory phenotype that might suppress antitumor immune responses. However, for a better understanding of the roles of $CD4^+$ $CD25^+$ T cells during MDV pathogenesis, the cells to which purified vIL-8 bound need to be further characterized. A model of vIL-8 functions during MD pathogenesis is shown in Fig. 8.

In conclusion, we demonstrate that the secreted vIL-8 chemokine is involved in various stages of MDV infection and the development of disease, including establishment of virus infection via the natural route. In addition, we identified two novel target cells for vIL-8: B cells, which are the main substrate for lytic replication of MDV, and $CD4^+$ $CD25^+$ T cells, a putative target for MDV transformation.

ACKNOWLEDGMENTS

We thank Bernd Kaspers, Oscar Negrete, Benhur Lee, and Jean-Francois Vautherot for providing us with reagents for this study. We are grateful to Annachiara Greco and Inês Veiga for their assistance with animal experiments. We also thank the Institut für Geflügelkrankheiten, Freie Universität Berlin, for providing fresh chicken blood.

A.T.E. was supported by the ZIBI Graduate School Berlin and GRK 1121 awarded by the DFG.

In vivo experiments were approved by the Landesamt für Gesundheit und Soziales in Berlin (approval number G0026/08).

REFERENCES

1. **Anobile JM, et al.** 2006. Nuclear localization and dynamic properties of the Marek's disease virus oncogene products Meq and Meq/vIL8. J. Virol. **80**:1160–1166.
2. **Ausländer S.** 2007. Aufreinigung und Charakterisierung monoklonaler Antikörper gegen Ochratoxin B. Bachelor's thesis. Universität Konstanz, Constance, Germany.
3. **Baaten BJ, et al.** 2009. Early replication in pulmonary B cells after infection with Marek's disease herpesvirus by the respiratory route. Viral Immunol. **22**:431–444.
4. **Baigent SJ, Smith LP, Nair VK, Currie RJ.** 2006. Vaccinal control of Marek's disease: current challenges, and future strategies to maximize protection. Vet. Immunol. Immunopathol. **112**:78–86.
5. **Brown AC, et al.** 2006. Interaction of MEQ protein and C-terminal-binding protein is critical for induction of lymphomas by Marek's disease virus. Proc. Natl. Acad. Sci. U. S. A. **103**:1687–1692.
6. **Brown AC, et al.** 2009. Homodimerization of the Meq viral oncoprotein is necessary for induction of T-cell lymphoma by Marek's disease virus. J. Virol. **83**:11142–11151.
7. **Burgess SC, Davison TF.** 2002. Identification of the neoplastically transformed cells in Marek's disease herpesvirus-induced lymphomas: recognition by the monoclonal antibody AV37. J. Virol. **76**:7276–7292.
8. **Burgess SC, et al.** 2004. Marek's disease is a natural model for lymphomas overexpressing Hodgkin's disease antigen (CD30). Proc. Natl. Acad. Sci. U. S. A. **101**:13879–13884.
9. **Calnek BW.** 1986. Marek's disease—a model for herpesvirus oncology. Crit. Rev. Microbiol. **12**:293–320.
10. **Calnek BW.** 2001. Pathogenesis of Marek's disease virus infection. Curr. Top. Microbiol. Immunol. **255**:25–55.
11. **Calnek BW, Schat KA, Ross LJ, Shek WR, Chen CL.** 1984. Further characterization of Marek's disease virus-infected lymphocytes. I. In vivo infection. Int. J. Cancer **33**:389–398.
12. **Cui X, Lee LF, Reed WM, Kung HJ, Reddy SM.** 2004. Marek's disease virus-encoded vIL-8 gene is involved in early cytolytic infection but dispensable for establishment of latency. J. Virol. **78**:4753–4760.
13. **Guinamard R, et al.** 1999. B cell antigen receptor engagement inhibits stromal cell-derived factor (SDF)-1alpha chemotaxis and promotes protein kinase C (PKC)-induced internalization of CXCR4. J. Exp. Med. **189**:1461–1466.
14. **Gunn MD, et al.** 1998. A B-cell-homing chemokine made in lymphoid follicles activates Burkitt's lymphoma receptor-1. Nature **391**:799–803.
15. **Hamroun D, Desmet F, Lalande M.** 2010. Human Splicing Finder, version 2.4.1. http://www.umd.be/HSF/.
16. **Jarosinski K, Kattenhorn L, Kaufer B, Ploegh H, Osterrieder N.** 2007. A herpesvirus ubiquitin-specific protease is critical for efficient T cell lymphoma formation. Proc. Natl. Acad. Sci. U. S. A. **104**:20025–20030.
17. **Jarosinski KW, et al.** 2007. Horizontal transmission of Marek's disease virus requires US2, the UL13 protein kinase, and gC. J. Virol. **81**:10575–10587.
18. **Jarosinski KW, Osterrieder N, Nair VK, Schat KA.** 2005. Attenuation of Marek's disease virus by deletion of open reading frame RLORF4 but not RLORF5a. J. Virol. **79**:11647–11659.
19. **Jarosinski KW, Schat KA.** 2007. Multiple alternative splicing to exons II and III of viral interleukin-8 (vIL-8) in the Marek's disease virus genome: the importance of vIL-8 exon I. Virus Genes **34**:9–22.
20. **Jarosinski KW, Tischer BK, Trapp S, Osterrieder N.** 2006. Marek's disease virus: lytic replication, oncogenesis and control. Expert Rev. Vaccines **5**:761–772.
21. **Kaiser P, et al.** 2005. A genomic analysis of chicken cytokines and chemokines. J. Interferon Cytokine Res. **25**:467–484.
22. **Kaiser P, et al.** 2009. Prospects for understanding immune-endocrine interactions in the chicken. Gen. Comp. Endocrinol. **163**:83–91.
23. **Kaufer BB, Jarosinski KW, Osterrieder N.** 2011. Herpesvirus telomeric repeats facilitate genomic integration into host telomeres and mobilization of viral DNA during reactivation. J. Exp. Med. **208**:605–615.
24. **Levy AM, et al.** 2005. Marek's disease virus Meq transforms chicken cells via the v-Jun transcriptional cascade: a converging transforming pathway for avian oncoviruses. Proc. Natl. Acad. Sci. U. S. A. **102**:14831–14836.
25. **Liu JL, Ye Y, Lee LF, Kung HJ.** 1998. Transforming potential of the herpesvirus oncoprotein MEQ: morphological transformation, serum-independent growth, and inhibition of apoptosis. J. Virol. **72**:388–395.
26. **Lupiani B, et al.** 2004. Marek's disease virus-encoded Meq gene is involved in transformation of lymphocytes but is dispensable for replication. Proc. Natl. Acad. Sci. U. S. A. **101**:11815–11820.
27. **Negrete OA, et al.** 2005. EphrinB2 is the entry receptor for Nipah virus, an emergent deadly paramyxovirus. Nature **436**:401–405.
28. **Osterrieder N.** 1999. Sequence and initial characterization of the U(L)10 (glycoprotein M) and U(L)11 homologous genes of serotype 1 Marek's disease virus. Arch. Virol. **144**:1853–1863.
29. **Osterrieder N, Kamil JP, Schumacher D, Tischer BK, Trapp S.** 2006. Marek's disease virus: from miasma to model. Nat. Rev. Microbiol. **4**:283–294.
30. **Parcells MS, et al.** 2001. Marek's disease virus (MDV) encodes an interleukin-8 homolog (vIL-8): characterization of the vIL-8 protein and a vIL-8 deletion mutant MDV. J. Virol. **75**:5159–5173.
31. **Qian Z, Brunovskis P, Lee L, Vogt PK, Kung HJ.** 1996. Novel DNA binding specificities of a putative herpesvirus bZIP oncoprotein. J. Virol. **70**:7161–7170.
32. **Qian Z, Brunovskis P, Rauscher F, III, Lee L, Kung HJ.** 1995. Transactivation activity of Meq, a Marek's disease herpesvirus bZIP protein persistently expressed in latently infected transformed T cells. J. Virol. **69**:4037–4044.
33. **Schat KA, Calnek BW, Fabricant J.** 1981. Influence of the bursa of Fabricius on the pathogenesis of Marek's disease. Infect. Immun. **31**:199–207.
34. **Schumacher D, Tischer BK, Fuchs W, Osterrieder N.** 2000. Reconstitution of Marek's disease virus serotype 1 (MDV-1) from DNA cloned as a bacterial artificial chromosome and characterization of a glycoprotein B-negative MDV-1 mutant. J. Virol. **74**:11088–11098.
35. **Schumacher D, Tischer BK, Trapp S, Osterrieder N.** 2005. The protein encoded by the US3 orthologue of Marek's disease virus is required for efficient de-envelopment of perinuclear virions and involved in actin stress fiber breakdown. J. Virol. **79**:3987–3997.
36. **Shack LA, Buza JJ, Burgess SC.** 2008. The neoplastically transformed (CD30hi) Marek's disease lymphoma cell phenotype most closely resembles T-regulatory cells. Cancer Immunol. Immunother. **57**:1253–1262.
37. **Shanmugasundaram R, Selvaraj RK.** 2011. Regulatory T cell properties of chicken CD4+CD25+ cells. J. Immunol. **186**:1997–2002.
38. **Staeheli P, Puehler F, Schneider K, Gobel TW, Kaspers B.** 2001. Cytokines of birds: conserved functions—a largely different look. J. Interferon Cytokine Res. **21**:993–1010.
39. **Tischer BK, et al.** 2005. High-level expression of Marek's disease virus glycoprotein C is detrimental to virus growth in vitro. J. Virol. **79**:5889–5899.
40. **Tischer BK, von Einem J, Kaufer B, Osterrieder N.** 2006. Two-step red-mediated recombination for versatile high-efficiency markerless DNA manipulation in Escherichia coli. Biotechniques **40**:191–197.
41. **Van de Walle GR, May ML, Sukhumavasi W, von Einem J, Osterrieder N.** 2007. Herpesvirus chemokine-binding glycoprotein G (gG) efficiently inhibits neutrophil chemotaxis in vitro and in vivo. J. Immunol. **179**:4161–4169.
42. **Witter RL, Calnek BW, Buscaglia C, Gimeno IM, Schat KA.** 2005. Classification of Marek's disease viruses according to pathotype: philosophy and methodology. Avian Pathol. **34**:75–90.